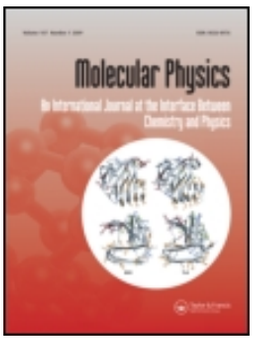

Taylor & Francis
Taylor & Francis Group

Molecular Physics

An International Journal at the Interface Between Chemistry and Physics

ISSN: 0026-8976 (Print) 1362-3028 (Online) Journal homepage: https://www.tandfonline.com/loi/tmph20

Conical intersections and double excitations in time-dependent density functional theory

Benjamin G. Levine , Chaehyuk Ko , Jason Quenneville & Todd J. MartÍnez

To cite this article: Benjamin G. Levine , Chaehyuk Ko , Jason Quenneville & Todd J. MartÍnez (2006) Conical intersections and double excitations in time-dependent density functional theory, Molecular Physics, 104:5-7, 1039-1051, DOI: 10.1080/00268970500417762

To link to this article: https://doi.org/10.1080/00268970500417762

Molecular Physics, Vol. 104, Nos. 5–7, 10 March–10 April 2006, 1039–1051

Taylor & Francis
Taylor & Francis Group

Conical intersections and double excitations in time-dependent density functional theory†

BENJAMIN G. LEVINE, CHAEHYUK KO, JASON QUENNEVILLE and TODD J. MARTÍNEZ*

Department of Chemistry, The Beckman Institute, and The F. Seitz Materials Research Laboratory, University of Illinois at Urbana-Champaign, Urbana, IL 61801, USA

(*Received 27 April 2005; in final form 12 May 2005*)

There is a clear need for computationally inexpensive electronic structure theory methods which can model excited state potential energy surfaces. Time-dependent density functional theory (TDDFT) has emerged as one of the most promising contenders in this context. Many previous tests have concentrated on vertical excitation energies, which can be compared to experimental absorption maxima. Here, we focus attention on more global aspects of the resulting potential energy surfaces, especially conical intersections which play a key role in photochemical mechanisms. We introduce a new method for minimal energy conical intersection (MECI) searches which does not require knowledge of the non-adiabatic coupling vector. Using this new method, we compute MECI geometries with multi-state complete active space perturbation theory (MS-CASPT2) and TDDFT. We show that TDDFT in the linear response and adiabatic approximations can predict MECI geometries and energetics quite accurately, but that there are a number of qualitative deficiencies which need to be addressed before TDDFT can be used routinely in photochemical problems.

1. Introduction

The accurate calculation of electronically excited states for large molecules remains a major challenge. At the same time, density functional theory (DFT) has emerged as a powerful method for computing potential energy surfaces of ground electronic states. Hence, it is natural to investigate the possibility of a density functional theory for excited electronic states. The time-dependent DFT (TDDFT) method has been developed for precisely this purpose [1–5], determining excited state energies through a response formalism which avoids the direct computation of wavefunctions for electronically excited states. Many previous studies have shown that TDDFT is competitive with the best wavefunction-based methods in the accurate prediction of vertical excitation energies [6–9]. Problems with accurate description of vertical excitation energies to Rydberg states have been noted and at least partially solved [8, 10–12]. The successes of TDDFT with respect to vertical excitation energies predominantly concern states which are singly-excited relative to the ground state. There remains some controversy regarding the ability of TDDFT to describe states with double-excitation character [13–15], and it is now widely agreed that the method (at least with presently-available functionals) fails to correctly describe excited states with significant charge transfer character [8, 16–19].

Relatively little work has investigated the accuracy of TDDFT for global excited state potential energy surfaces [20, 21]. The question of whether TDDFT is able to describe doubly-excited states is of particular importance here. Even when the initially-excited state is dominated by single excitations, the propensity for curve crossing in the excited state manifold makes it unlikely that the global potential energy surface could be well described by a method which does not treat doubly-excited states correctly. For example, the low-lying bright electronic state in ethylene is a $\pi \rightarrow \pi^*$ excitation, but as the molecule relaxes on the excited state, it acquires significant double excitation character [22].

A further question is the ability of TDDFT to describe conical intersections—molecular geometries where two electronic states are exactly degenerate. Conical intersections (CIs) are now recognized to play a critical role in the reaction dynamics of electronic excited states [23–26]. State-averaged [27] complete

*Corresponding author. Email: tjm@spawn.scs.uiuc.edu

†Dedicated to Professor M. A. Robb on the occasion of his 60th birthday.

Molecular Physics
ISSN 0026–8976 print/ISSN 1362–3028 online
http://www.tandf.co.uk/journals
DOI: 10.1080/00268970500417762

active space self-consistent field [28] (SA-CASSCF) have seen considerable application to the description of conical intersection geometries and energetics [29–35], and have also been compared to methods including dynamical electron correlation such as multi-reference single- and double-excitation configuration interaction (MRSDCI) or second-order perturbation theory (CASPT2) [36]. In many cases, SA-CASSCF compares favourably to the more accurate MRSDCI and CASPT2 methods. However, one should not expect good agreement in cases where charge transfer is important, since ionic states are often strongly stabilized by dynamical electron correlation. The availability of analytic gradients and non-adiabatic coupling terms along with the ability to provide a reasonable global potential energy surface make SA-CASSCF one of the methods of choice for first-principles dynamics studies of photochemistry, where the potential energy surfaces and couplings are computed 'on the fly'. Robb and co-workers have exploited this in several studies [37, 38] using surface-hopping methods [39, 40] to represent the electronic state crossing which occurs when CIs are encountered. We have used both CASSCF and MRSCI methods in the *ab initio* multiple spawning (AIMS) method [26, 41–45], which solves the electronic and nuclear Schrödinger equations simultaneously in order to include the effects of breakdown of the Born–Oppenheimer approximation. Often, a careful choice of active space and number of electronic states included in the averaging procedure can lead to improved agreement with MRSDCI and CASPT2 results over a broad range of the potential energy surfaces. However, it would be preferable to include the dynamic correlation energy explicitly in AIMS calculations. We have done this using equation-of-motion coupled-cluster theory, concentrating on the excited state dynamics before conical intersections are encountered [46, 47]. It is clear that TDDFT would provide a much more economical alternative, with possible application to very large molecules.

It is especially important at this point to note that the time dependence referred to in TDDFT is usually *not* time dependence of the nuclei. Instead, it is the time dependence of the electrons when the *fixed* nuclear framework is subject to a periodic radiation field. In the linear-response matrix formulation, as summarized below, even the time dependence of the electrons is obscured by transforming to the frequency domain. There is some work aimed at formulating TDDFT for explicit time dependence of both nuclei and electrons [48]. However, this is still at an early stage and we will not consider it further.

This paper begins with a brief summary of TDDFT in the linear-response regime using the adiabatic approximation and the relationship to single-excitation configuration interaction (CIS) methods [49]. Then, we comment on the performance of TDDFT for doubly-excited states. We show that the lowest-lying doubly-excited state is in fact completely absent in both ethylene and butadiene. We then investigate the performance of TDDFT for the chromophore of photoactive yellow protein (PYP) along a coordinate-driving path determined using SA-CASSCF. TDDFT and CASPT2 are shown to agree very well. Given our results for ethylene and butadiene, one can conclude that this is due to the fact that the S_1 state in PYP chromophore is always well represented as a single excitation from S_0. The good agreement we obtain for PYP chromophore emboldens us to devise a method for optimizing minimal energy CIs (MECIs) in TDDFT and make direct comparisons with MECI geometries and energetics determined with the multi-state analogue [50] of CASPT2 (MS-CASPT2). Again, excellent agreement is observed. However, we then investigate the topography of the potential energy surfaces in the vicinity of the MECIs and show that in fact there are no *conical* intersections between the reference and response states in TDDFT. This is explained by analogy to CIS. We conclude with some discussion of the problems and prospects for TDDFT in the context of molecular photochemistry.

2. Theory

The TDDFT method is based on the Runge–Gross theorem [5], which is the analogue of the Hohenberg–Kohn theorem [51] in ground state DFT. The basic principle is very similar to ground state DFT—namely that a time-dependent system of interacting electrons can be mapped onto a model time-dependent system of non-interacting electrons with the same one-electron density as the true interacting system. This mapping occurs via a time-dependent density functional which should depend on the initial state [52] and furthermore should be temporally non-local [53]. The resulting time-dependent Kohn–Sham equations are

$$i\frac{\partial}{\partial t}\varphi(r,t) = \left(-\frac{\nabla^2}{2} + v_{\mathrm{KS}}(r,t)\right)\varphi(r,t), \tag{1}$$

$$v_{\mathrm{KS}}(r,t) = v_{\mathrm{e}}(r,t) + \int \mathrm{d}^3 r' \frac{\rho(r',t)}{|r-r'|} + \frac{\delta A_{\mathrm{xc}}[\rho]}{\delta\rho(r,t)}, \tag{2}$$

where δ denotes functional differentiation and $v_{\mathrm{e}}(r,t)$ is the time-dependent external potential (usually including the electron–nuclear and matter–radiation interactions). The second term in equation (2) approximates

the electron–electron repulsion, and the third term contains the unknown action functional which maps the solutions of equation (1) onto the solutions of the full time-dependent Schrödinger equation. As in the time-independent ground state Kohn–Sham method, the density is given by the appropriate sum of the squares of orbitals $\varphi(r,t)$. In practice, the adiabatic approximation is often invoked whereby both the initial state-dependence and temporal non-locality of $A_{\mathrm{xc}}[\rho]$ are ignored, i.e.

$$\frac{\delta A_{\mathrm{xc}}[\rho]}{\delta\rho(r,t)} \approx \frac{\delta E_{\mathrm{xc}}[\rho_t]}{\delta\rho_t(r)}. \tag{3}$$

This amounts to using the ground state exchange-correlation functional E_{xc}, for which many approximations have been developed, in place of the unknown action functional. Since this replacement is exact when the external potential is time independent, one can argue that it should be a reasonable approximation when the external potential is only weakly time dependent.

Casida has developed an energy-domain matrix formulation of adiabatic TDDFT within the linear-response approximation [4]. This is especially convenient for implementation in the framework of quantum chemistry, and Hirata and Head-Gordon have shown that it closely parallels CIS [54]. The linear-response approximation is equivalent to first-order time-dependent perturbation theory and hence should be valid for weak external radiation fields. To summarize briefly, the electronic excitation energies of a molecule are identified with the poles of the frequency-dependent polarizability [4]. Introducing a basis set, one can cast this as an eigenvalue problem [4, 55]:

$$\begin{pmatrix} \mathbf{A} & \mathbf{B} \\ \mathbf{B} & \mathbf{A} \end{pmatrix}\begin{pmatrix} \mathbf{X} \\ \mathbf{Y} \end{pmatrix} = \omega\begin{pmatrix} 1 & 0 \\ 0 & -1 \end{pmatrix}\begin{pmatrix} \mathbf{X} \\ \mathbf{Y} \end{pmatrix}, \tag{4}$$

where

$$A_{ai\sigma,bj\tau} = \delta_{\sigma\tau}\delta_{ij}\delta_{ab}(\varepsilon_{a\sigma} - \varepsilon_{i\sigma}) + K_{ai\sigma,bj\tau}, \tag{5}$$

$$B_{ai\sigma,bj\tau} = K_{ai\sigma,jb\tau}, \tag{6}$$

$$K_{kl\sigma,mn\tau} = \int \mathrm{d}^3r, \mathrm{d}^3r' \phi^*_{k\sigma}(r)\phi_{l\sigma}(r) \times \left(\frac{1}{|r-r'|} + \frac{\delta^2 E_{\mathrm{xc}}}{\delta\rho_\sigma(r)\delta\rho_\tau(r)}\right)\phi^*_{n\tau}(r')\phi_{m\tau}(r'), \tag{7}$$

where σ and τ label the orbital spin. The labels i, j and a, b represent occupied and virtual orbitals, respectively, and the elements X_{ai} and Y_{ai} represent the coefficients describing the change induced in the density associated with the orbital products $\varphi_a\varphi_i^*$ and $\varphi_i\varphi_a^*$. Note that K is essentially a two-electron integral between KS orbitals including a correction from the correlation functional. Hirata and Head-Gordon showed that the Tamm–Dancoff approximation, which amounts to ignoring $\mathbf{Y}$ in equation (4), can often accurately reproduce the results of TDDFT [54]. Within the Tamm–Dancoff approximation, the problem reduces to the eigenvalue equation (now of half the matrix dimension):

$$\mathbf{AX} = \omega\mathbf{X}. \tag{8}$$

This is strongly reminiscent of the eigenvalue problem solved in CIS:

$$(\mathbf{H} - E_0)\mathbf{X} = \omega\mathbf{X}, \tag{9}$$

$$(H - E_0)_{ia\sigma,jb\tau} = \delta_{\sigma\tau}\delta_{ij}\delta_{ab}(\varepsilon_{a\sigma} - \varepsilon_{i\sigma}) + \langle i_\sigma b_\tau || a_\sigma j_\tau \rangle. \tag{10}$$

The only difference is the replacement of the antisymmetrized two-electron integral in equation (10) with the K term in equation (7), which substitutes the exchange-correlation functional for the exchange operator.

The formal similarity between CIS and TDDFT/TDA and the observed agreement between TDDFT/TDA and TDDFT suggest that TDDFT may have some of the deficiencies of CIS, at least with the current array of functionals and within the linear response and adiabatic approximations. In particular, CIS only reproduces states which are predominantly singly-excited in character and can only produce qualitatively correct results in regions of the potential energy surface where the ground state is accurately modelled as a single determinant. However, the situation is not entirely clear, and promising numerical results have led to the suggestion that doubly excited states may sometimes be correctly modelled with adiabatic linear-response TDDFT [15].

3. Double excitations in TDDFT

Ethylene and butadiene provide a useful testbed for empirical answers to the questions concerning the applicability of TDDFT for states with significant double excitation character. After $\pi \rightarrow \pi^*$ excitation in ethylene, the molecule twists about the C=C bond and subsequently pyramidalizes about one of the carbon atoms [22, 26, 56]. The natural diabatic description of the low-lying electronic states in ethylene [57] is based on two electrons in two orbitals leading to three orbital occupation patterns—$\pi\pi$, $\pi\pi^*$ and $\pi^*\pi^*$. The PES corresponding to the $\pi\pi^*$ configuration (which is the dominant component of the bright electronic state)

is expected to have a minimum with 90° torsion about the C=C double bond. The $\pi^*\pi^*$ state (doubly excited relative to the $\pi\pi$ ground state) has significant charge transfer character and is thus expected to exhibit a minimum at a twisted geometry with pyramidalization about one of the carbon atoms. In actuality, the global minimum on S_1 is of doubly-excited character, leading to an S_1 minimum which is both twisted and pyramidalized. However, if the doubly-excited state were completely absent over the whole range of twisting and pyramidalization, the minimum energy S_1 geometry would be purely twisted. We calculate the ground and valence excited state potential energy surfaces in these two internal coordinates here using CIS, TDDFT, and CASPT2 and the 6-31G* basis set. Geometries are obtained as in our previous work [26, 58]. The version of CASPT2 used is quasi-degenerate perturbation theory as implemented in GAMESS [59], while the CIS/TDDFT calculations are carried out using spin-restricted Hartree–Fock/Kohn–Sham as implemented in Gaussian 98 [60]. In figure 1(a), we show the form of the S_0 and S_1 potential energy surfaces (PESs) obtained from CASPT2. The S_1 minimum occurs at a twisted and pyramidalized geometry, and can be seen to be in close energetic and geometric proximity to an S_0/S_1 conical intersection. The S_1 PES is shown in contour representation in figure 1(b), which highlights the twisted and pyramidalized character of the minimum. Using TDDFT, the minimum is found at a purely twisted geometry with no pyramidalization, as expected if the doubly-excited state were not being represented. For comparison, the CIS S_1 PES is shown in figure 1(d). The form of the CIS and TDDFT S_1 PESs is very similar. Although the strong similarity of the TDDFT and CIS S_1 PESs suggests that TDDFT cannot model the doubly-excited state, an alternative explanation which cannot be ruled out is that the doubly-excited state lies too high because of its charge transfer character. However, the general tendency in TDDFT is the opposite—overstabilization of charge transfer states. Thus, this explanation seems unlikely [17].

The *trans* form of butadiene has two low-lying, near-degenerate valence singlet excited states. These are of B_u and A_g symmetry, and there has been a long controversy concerning which is lower in energy. The most sophisticated treatments [61, 62] seem to indicate that the B_u state lies below the A_g state, but it is likely not presently justified to say anything more than that they are within 0.2 eV of each other. The A_g state is found in wavefunction-based treatments to have considerable double-excitation character and thus it was quite surprising when Hsu *et al.* reported that this state seemed to be correctly described by TDDFT [15]. The correspondence of the states was based on wavefunction symmetry and comparisons of the excitation energies and the spatial extent of the electronic wavefunction to *ab initio* results including dynamic electron correlation such as EOM-CCSD and CASPT2. Cave *et al.* later speculated [14, 63] that the state which Hsu *et al.* labelled as ^1A_g was actually a Rydberg state and that deficiencies of TDDFT in treating Rydberg states were the cause of the appearance of this state in the energy region where the valence state was expected. There is some evidence for such an explanation in the original paper of Hsu *et al.*—the excitation energy of the 'valence' A_g state drops by 0.5 eV when the basis set is extended to include two sets of diffuse functions. However, the explanation is not entirely satisfactory. As Hsu *et al.* argued, the spatial extent of the putative valence ^1A_g state is valence-like and quite far outside the range expected for a Rydberg state.

In an attempt to settle the question of the character of the ^1A_g state produced by TDDFT, we have mapped out the excited state PESs for *trans*-butadiene along the bond-alternation coordinate. This is expected from *ab initio* methods to be the dominant initial relaxation coordinate after excitation to the ^1B_u state, and serves as a sensitive diagnostic of the valence excited state character—the PES for a Rydberg-like state will be quite flat with respect to this distortion. In figure 2, we compare the TDDFT and CASPT2 results, where the bond alternation coordinate is defined as simultaneous and equal stretching/compression of the C–C bonds as indicated in the inset. The reference structure (bond alternation of zero) is the S_0 minimum as determined using BLYP and the 6-31G basis set. For ease of comparison, we have defined the zero of energy to be the ^1B_u state energy at the Franck–Condon point (the CASPT2 and TDDFT vertical excitation energies are 6.42 and 5.89 eV, respectively). The B3LYP functional is used for TDDFT and the intuitive active space (four electrons in four orbitals) is used in CASPT2 with orbitals determined from equal weighting of the lowest five singlet states in CASSCF, i.e. SA-5-CAS(4/4)-PT2.The CASPT2 variant used here is the contracted version implemented in MolPro [64]. In both cases, the 6-31G** basis set is used. There is almost quantitative agreement between CASPT2 and TDDFT for the ^1B_u state. However, the distinguishing characteristic of the 2^1A_g state in CASPT2 is that it favours greater bond alternation than the ^1B_u state, as should be expected given its double excitation character and hence lower bond order. The 2^1A_g state from TDDFT is similar to the ^1B_u state in this regard and it does not seem reasonable to identify it with the 2^1A_g state from CASPT2. In fact, it is more similar to the 3^1Ag state of CASPT2, as is clearly seen when the curve is

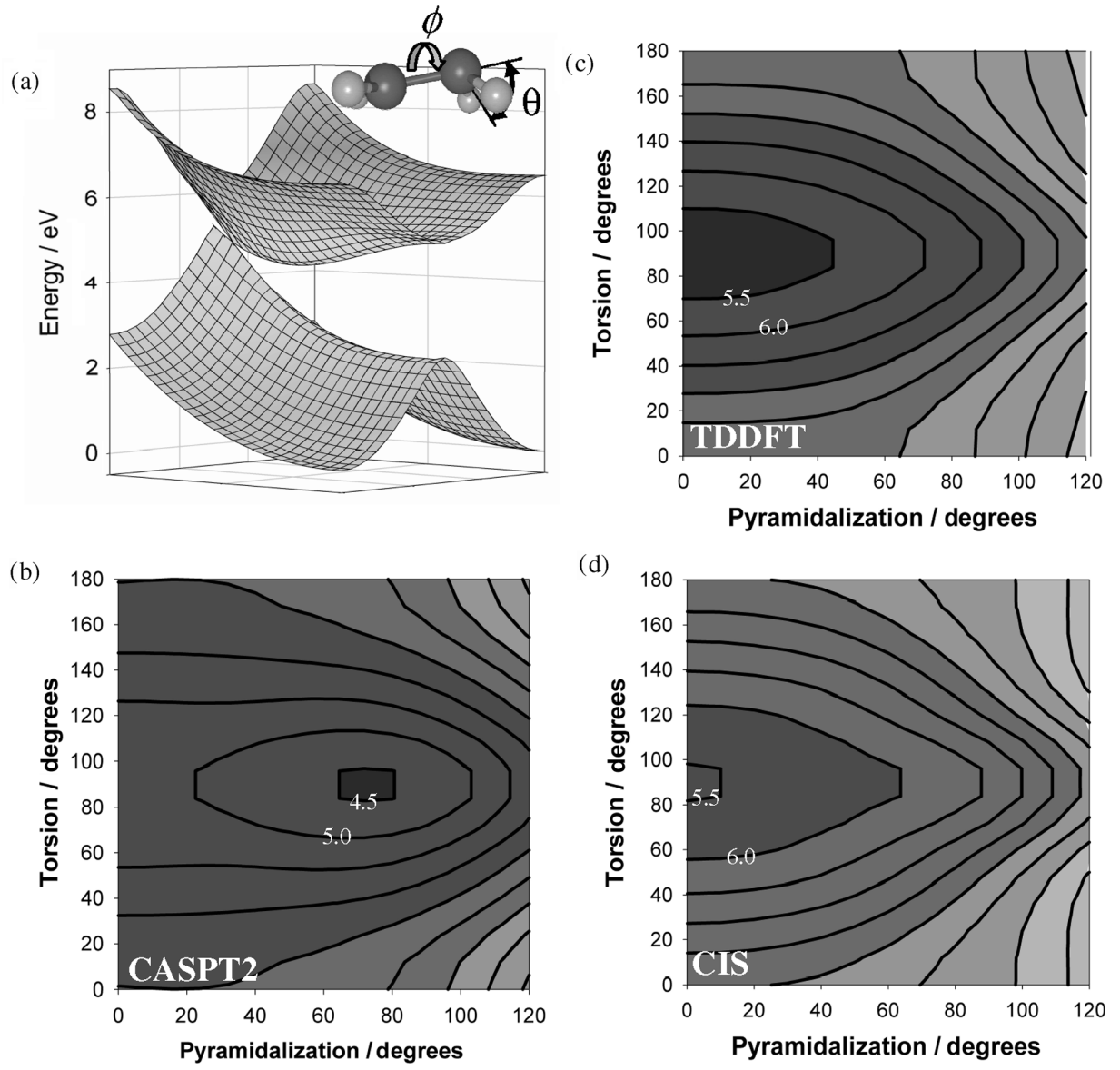

Figure 1. Important features of ground and excited PESs for ethylene photodynamics and demonstration of the inadequacy of TDDFT and CIS methods for this problem. The upper left panel (a) shows S_0 and S_1 PESs for ethylene in the pyramidalization and torsion coordinates (defined in the inset) which dominate the photodynamics. This surface was calculated using quasidegenerate multi-reference perturbation theory—CAS(2/2)*QDPT2. The global minimum on S_1 occurs at twisted *and* pyramidalized geometries. Subsequent panels (b)–(d) provide a quantitative comparison of the S_1 PES obtained with CAS(2/2)*QDPT2, TDDFT/B3LYP and CIS, respectively. All calculations use the 6-31G* basis set. The TDDFT and CIS calculations are performed in a spin-restricted formalism. Contour values are given in eV and in all cases the energies are referenced to the S_0 equilibrium geometry at the corresponding level of theory. Only the multi-reference calculation captures the S_1 minimum correctly.

shifted as shown by the hatched squares. There is an avoided crossing between the CASPT2 4^1A_g and 3^1A_g states which TDDFT does not describe correctly. This is to be expected because the 4^1A_g state in CASPT2 again has significant double excitation character.

The above results make it clear that double excitations are completely absent in TDDFT when the linear response and adiabatic approximations are used. An approach which goes beyond the adiabatic approximation to include double excitations has been proposed and seems quite promising [13, 14]. However, there are many cases where the interesting excited state is always well described as a single excitation. It is interesting to gain more experience with the accuracy of these singly excited states by comparing TDDFT and CASPT2. One of the molecules we have been interested in recently

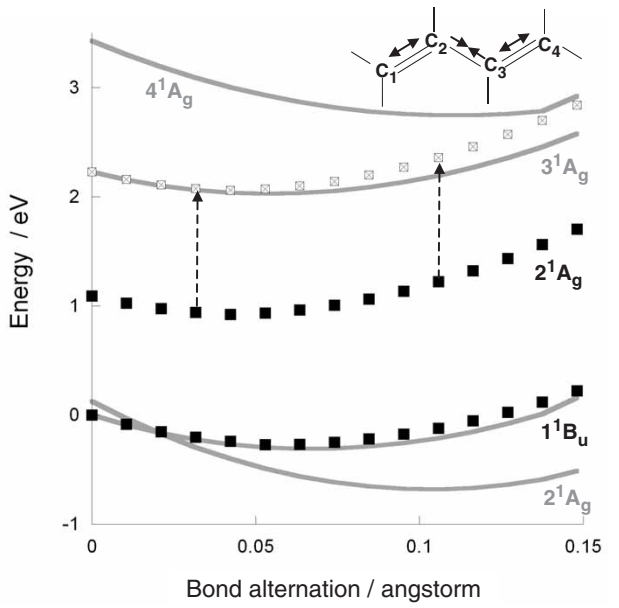

Figure 2. Energy as a function of bond alternation coordinate (depicted in the inset) for the first several excited states of *trans*-butadiene using TD-B3LYP (black squares) and SA5-CAS(4/4)*PT2 (grey solid lines) methods, using the 6-31G** basis set. To facilitate comparison, the zero of energy is chosen as the S_1 energy at the Franck–Condon point. The 2^1A_g and 4^1A_g states as determined by CASPT2 have significant double excitation character. While the 1^1B_u energy curves from TDDFT and CASPT2 are in excellent agreement, the 2^1A_g curves are not. In fact, the 2^1A_g state from TDDFT is more similar in behaviour to the 3^1A_g state from CASPT2. This is highlighted by shifting the TDDFT 2^1A_g state (hatched open squares). This suggests that TDDFT with the current array of approximate functionals is incapable of reproducing the state with significant doubly excited character.

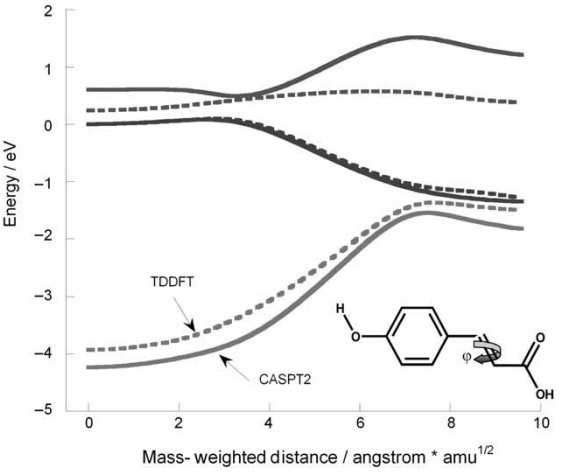

Figure 3. Comparison of TDDFT-B3LYP (dotted lines) and CASPT2 (solid lines) for the three lowest singlet electronic states of a PYP chromophore analogue along a coordinate-driving path on S_1. Geometries are obtained by minimizing the energy on S_1 using a CASSCF(6/5) wavefunction subject to fixed dihedral angle φ (defined using only carbon atoms) varying from 180° (left side) to 70°. In all cases, the 6-31G* basis set is used. The zero of energy is chosen in both cases as the S_1 energy at the *trans* S_1 minimum. Notice the exceptionally good agreement between TDDFT and CASPT2 for S_0 and S_1. However, also note that S_2 is not well represented by TDDFT, especially to the right of the S_1 torsion barrier, where CASSCF predicts that S_2 has significant double excitation character.

is an analogue of the chromophore in photoactive yellow protein (PYP). Since we have already determined a minimal energy coordinate driving path on S_1 for this molecule with CASSCF and the S_1 wavefunction is dominated by a single excitation, this is a convenient choice for such a test. The relevant coordinate is torsion about a C=C double bond, as shown in the inset to figure 3. All other internal coordinates are relaxed to minimize the energy for each fixed value of the indicated torsion angle. More information is available in our previous work, where we have first reported the CASSCF and CASPT2 results [43]. In figure 3, we compare CASPT2 and TDDFT using the B3LYP functional. Both calculations use the 6-31G* basis set and the geometries were determined using CASSCF. The agreement between TDDFT and CASPT2 for the S_1 PES along this path is nearly quantitative. The only significant difference arises in the twisted region (near the right-hand side of the graph) where the S_0/S_1 gap is smaller in TDDFT. The difference is not really large enough to be able to state with confidence which of the two methods is more nearly correct. It would seem likely that both methods predict that there are low-lying conical intersections near the twisted geometry. This leads us to investigate conical intersection geometries in TDDFT.

4. Conical intersections in TDDFT

Most algorithms for MECI searches require the energy difference gradient ($\mathbf{g}_{IJ}$) and non-adiabatic coupling ($\mathbf{h}_{IJ}$) vectors:

$$\mathbf{g}_{IJ} = \frac{\partial}{\partial \mathbf{R}}[E_I - E_J], \tag{11}$$

$$\mathbf{h}_{IJ} = \left\langle \psi_I \left| \frac{\partial}{\partial \mathbf{R}} \right| \psi_J, \right\rangle, \tag{12}$$

where $\mathbf{R}$ is the vector of nuclear coordinates. At a conical intersection geometry, these two directions define the branching plane in which the PESs for both the lower and upper adiabatic states I and J

are discontinuous. By limiting the search for a minimum to the directions perpendicular to the branching plane, one can apply traditional optimization methods which assume continuity of the underlying functions [65]. There are two objectives in a MECI search—minimization of the energy gap separating states and minimization of the energy of the upper state. These two objectives are usually combined using a Lagrange multiplier [66, 67]. Robb and co-workers introduced an easily-implemented method which keeps the Lagrange multiplier fixed [66]. However, application of this algorithm is not straightforward for TDDFT because the non-adiabatic coupling vector is required. Since the TDDFT method does not have explicit access to the wavefunctions for response states, it is not so clear how to obtain the non-adiabatic coupling vector. Several procedures have been described in the literature but not widely implemented [68, 69]. Here we present an algorithm which smoothes the derivative discontinuities and allows one to locate MECIs without knowledge of the non-adiabatic coupling vector. This method can be applied in any case where **h** is not easily calculated, for example TDDFT and CASPT2.

Our method is based on the penalty Lagrange multiplier technique [70] and begins with the pair of functions:

$$f_1(\mathbf{R}, \lambda_1) = E_J(\mathbf{R}) + \lambda_1 \Delta E(\mathbf{R}), \tag{13}$$

$$f_2(\mathbf{R}, \lambda_2) = \frac{E_J(\mathbf{R}) + E_I(\mathbf{R})}{2} + \lambda_2 \frac{\Delta E(\mathbf{R})^2}{(\Delta E(\mathbf{R}) + \alpha)}, \tag{14}$$

where state J is taken to be the upper state, $\Delta E(R)$ is the energy gap between states I and J, λ_i are Lagrange multipliers (with $\lambda_2 = 0.5 + \lambda_1$), and α is a numerical parameter. The important feature of equation (14) is that the average of the two electronic energies is continuous even in the vicinity of a conical intersection. We set α to 0.02 hartree in all of the calculations described here, but it can be tuned to improve convergence. When $f_1(\mathbf{R}, \lambda)$ is fully minimized with respect to $\mathbf{R}$ and stationary with respect to λ, we have reached a minimal energy intersection point, but $f_1(\mathbf{R}, \lambda)$ is not differentiable at the intersection point. The function $f_2(\mathbf{R}, \lambda)$ is differentiable as long as we are in the neighbourhood of at most a two-state intersection involving states I and J. Furthermore, it tends to $f_1(\mathbf{R}, \lambda)$ when the energy gap is large. Therefore, we first optimize $f_2(\mathbf{R}, \lambda)$ to get near the MECI. Then we optimize $f_1(\mathbf{R}, \lambda)$ to find a true MECI. In practice, we find that optimizing $f_1(\mathbf{R}, \lambda)$ after $f_2(\mathbf{R}, \lambda)$ generally does not change the result very much when compared to simply optimizing $f_2(\mathbf{R}, \lambda)$, but this will clearly depend on the value of the parameter α.

We have used the above procedure with MS-CASPT2 and numerical differentiation to optimize MECI geometries which might be relevant in the photoisomerization of *trans*-butadiene. We find three low-lying S_0/S_1 MECIs, all of which are twisted about the terminal C–C bond. Two of these also have considerable charge transfer character, as supported both by wavefunction analysis and pyramidalization about carbon atoms. These can be distinguished by whether the terminal methylene group about the twisted C–C bond is positively or negatively charged, and we denote them as Me^+ and Me^-. The third intersection (transoid MECI) does not exhibit significant charge transfer character and is essentially the MECI found and extensively discussed by Robb and co-workers [32, 71, 72]. In table 1, we present TDDFT and *ab initio* results for the S_0/S_1 energy gaps at these three MECIs and also for similar twisted/pyramidalized MECIs involved in photoisomerization of stilbene [73] and ethylene [22, 26, 56]. The stilbene and ethylene MECI optimizations were performed using SA-2-CAS(2/2) with the 6-31G** basis set. Notice that TDDFT with almost all functionals (the chosen set includes local,

Table 1. Comparison of S_0/S_1 energy gaps (eV) obtained with TDDFT (using different functionals) and *ab initio* methods at *ab initio*-optimized S_0/S_1 MECI geometries. Basis sets used are 6-31G unless otherwise specified. Butadiene MECI geometries were optimized using MS-CAS(4/4)-PT2 with the 6-31G** basis set. Stilbene and ethylene MECI geometries were optimized using SA-2-CAS(2/2) with the 6-31G** basis set. TDDFT tends to predict small energy gaps (those less than or equal to 0.3 eV are bold to guide the eye) at the *ab initio*-optimized MECI geometries, while CIS erroneously predicts large gaps.

	Butadiene				
	Me^+	Me^-	transoid	Stilbene	Ethylene
TDDFT					
LDA	**0.25**	**0.27**	0.34	**0.27**	**0.24**
BLYP	0.37	**0.21**	0.45	**0.19**	0.32
PW91	**0.30**	0.32	0.37	**0.23**	**0.25**
PBE	0.36	0.32	0.38	**0.23**	**0.28**
B3LYP	**0.10**	**0.09**	**0.03**	**0.25**	**0.10**
B3LYP/6-31G*	**0.21**	**0.29**	**0.03**	**0.01**	**0.09**
B3LYP/6-31G**	**0.21**	**0.30**	**0.03**	**0.03**	**0.06**
MPW1PW91	**0.15**	**0.06**	**0.21**	**0.13**	**0.22**
PBE1	**0.15**	**0.06**	**0.20**	**0.12**	**0.21**
Ab initio					
CIS	1.66	1.28	1.63	1.09	1.12
CIS/6-31G**	1.97	1.56	1.60	1.32	1.48
CASSCF	0.80	0.71	**0.20**	**0.27**	0.43
CASSCF/6-31G**	**0.30**	0.36	**0.24**	**0.00**	**0.00**
MS-CASPT2/6-31G**	**0.00**	**0.00**	**0.00**	0.53	**0.26**

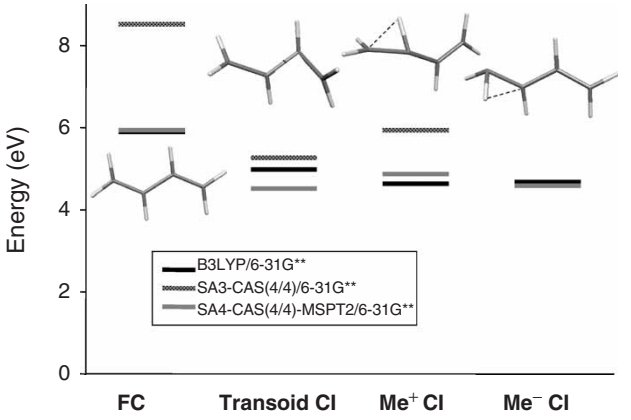

Figure 4. The energies of the Frank–Condon point and three S_0/S_1 MECIs of importance to the photodynamics of butadiene optimized at the B3LYP/6-31G** (black), SA3-CAS(4/4)/6-31G** (hatched), and SA4-CAS(4/4)-MSPT2/6-31G** (grey) levels of theory. All energies are relative to the S_0 energy at the Frank–Condon point at each respective level of theory. Despite significant effort we were unable to locate a Me^- conical intersection at the CAS(4/4) level of theory. Notice that the energies at the TDDFT level of theory agree well with from MS-CASPT2, in contrast to CASSCF.

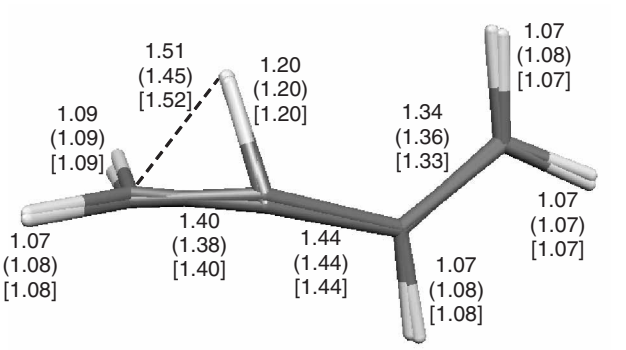

Figure 5. Comparison of MECI geometries for the Me^+ S_0/S_1 MECI of butadiene using B3LYP, SA-3-CASSCF(4/4) and SA-4-CAS(4/4)*MSPT2 electronic structure methods with the 6-31G** basis set. Bond lengths (Angstrom) are shown for B3LYP, CAS (in parenthesis) and MS-CASPT2 (in brackets). All three methods predict qualitatively similar MECI geometries.

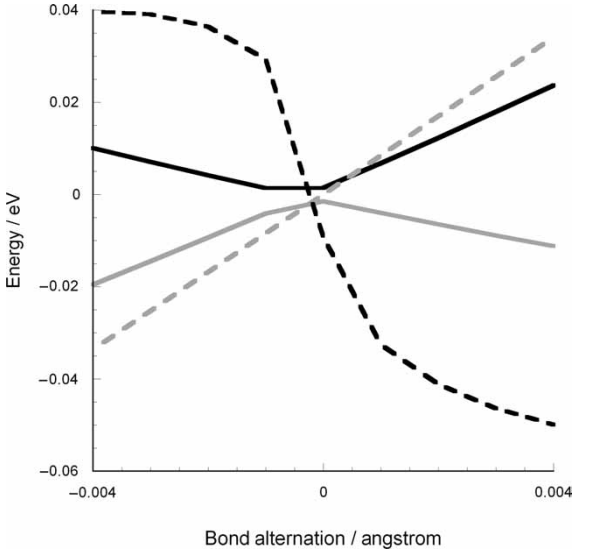

Figure 6. Behaviour of SA-3-CASSCF(4/4) (solid lines) and TDDFT (B3LYP, dashed lines) potential energy curves near the transoid MECI in butadiene. The distortion coordinate is bond alternation (as shown in figure 1) from the MECI structure, which corresponds approximately to the energy difference gradient in CASSCF. The grey and black lines denote S_0 and S_1, respectively, for the CASSCF potential energy curves. For TDDFT, the black line is the response state and the grey line is the reference (closed shell singlet) state. Note the rapid change in the TDDFT response state energy near the MECI, which is not supported by the *ab initio* results. Furthermore, the TDDFT response state becomes the ground state on the right side of the plot.

generalized gradient approximation and hybrid functionals) correctly predicts small energy gaps at the *ab initio*-optimized MECI geometries. In general, the hybrid functionals give lower energy gaps than the other functionals, suggesting that these functionals may produce more accurate results. The CIS method does not perform well, predicting energy gaps of more than 1 eV at each of the MECIs determined with CASSCF or MS-CASPT2.

The previous results encourage us to further optimize MECI geometries directly using TDDFT. We present the results of such optimization in figure 4, which shows the energies (relative to the S_0 minimum at each level of theory) for the B_u state at the Franck–Condon point and each of the three MECIs. Note that only one of the charge transfer MECIs (Me^+) could be located using SA-3-CASSCF(4/4), despite repeated and extensive effort. There is excellent agreement between TDDFT and MS-CASPT2—much better than the agreement between CASSCF and MS-CASPT2. This agreement extends also to the molecular geometries, as shown for a representative case (the Me^+ S_0/S_1 MECI) in figure 5.

The shape of the PESs in the region around a MECI can have a large effect on the propensity of electronic quenching [38, 43, 74–76]. Thus, we now ask about the accuracy of TDDFT in this respect. Figure 6 compares cuts of the potential energy surface along the bond alternation coordinate (as defined in figure 1) for the transoid MECI of butadiene. The bond alternation coordinate is approximately the energy difference gradient vector as determined by CASSCF. The agreement is not very good, and in fact the TDDFT curve appears to vary much more rapidly than one would

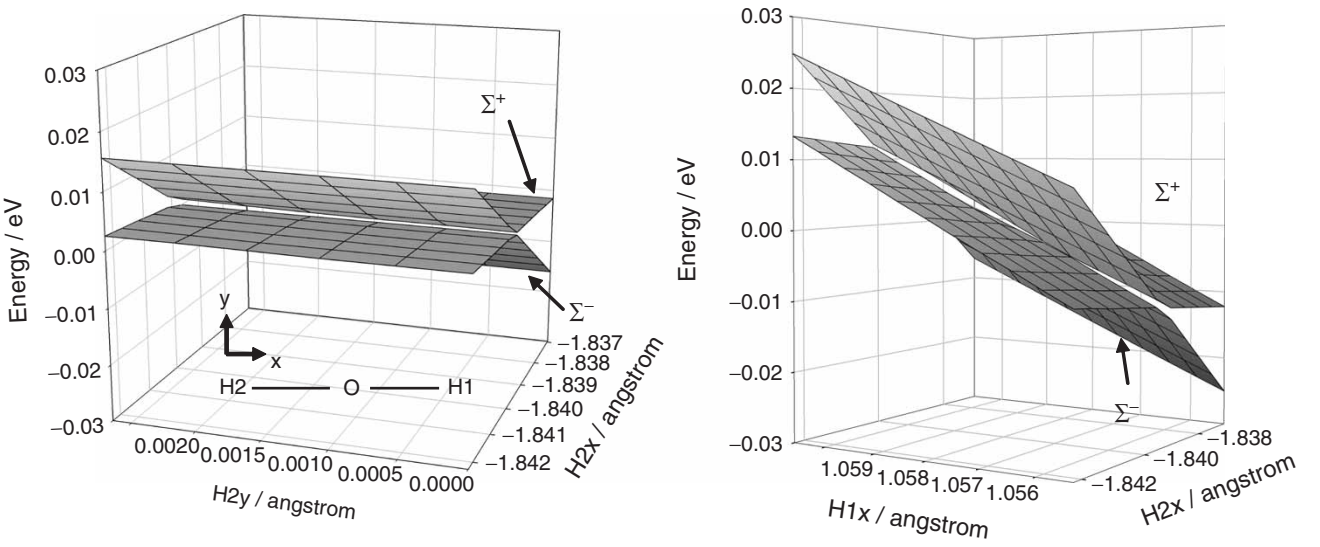

Figure 7. Potential energy surfaces of H_2O in the region surrounding a linear surface intersection calculated using CIS/6-31G. Only one of the three independent displacement coordinates splits the degeneracy. More accurate electronic structure treatments (see figure 8) predict that this intersection is conical and therefore has two branching directions.

expect in the region very close to the MECI. Furthermore, this plot highlights that the response state can become the ground state, i.e. the excitation energy from TDDFT can be negative. This arises because we use spin-restricted DFT and one of the two states involved in the intersection is closed-shell while the other is an open-shell singlet. Hence, the 'ground' state (the reference state from which response is calculated) must always be the closed-shell state. Essentially, TDDFT is restricted to a diabatic labelling of the states in this case. Thus, an exact functional must map the density generated from the closed-shell wavefunction into the energy of the open-shell wavefunction in some regions of the PES and into the energy of the closed-shell wavefunction in others. It seems unlikely that this could be accomplished unless the functional uses information from both states. One possible solution to this problem would be the use of a spin-unrestricted wavefunction in the Kohn–Sham procedure. In the case of butadiene, this is not successful because of severe spin-contamination problems. However, we comment on this possibility further below.

One may suspect that the diabatic nature of the TDDFT states will lead to an incorrect dimensionality of the branching plane in which the degeneracy is lifted around a CI. In particular, the dimensionality of the degenerate space around a CI should be $N-2$ while the corresponding dimensionality for the crossing of diabatic surfaces should be $N-1$, where N is the number of internal degrees of freedom [77]. It is best to investigate this in a molecule with few degrees of freedom, so that the behaviour of the PESs in all dimensions can be explored. Thus, we turn to H_2O as a simple test case. There is a conical intersection in a linear geometry, which we focus on here. The 'diabatic' behaviour observed originates in the restrictions imposed on the wavefunction which represents the ground state. Hence, similar behaviour can also be expected in CIS and it is useful to compare CIS and TDDFT. In figure 7, we show the S_0 and S_1 PESs for a water molecule in the region surrounding the linear conical intersection using the CIS wavefunction. The coordinate axes correspond to Cartesian displacements of the hydrogen atoms, and between the left and right panel, all internal degrees of freedom are exhausted. The important point is that the degeneracy between the intersecting states is lifted only along one dimension, as is expected in a case where the two states are forbidden from interacting at any geometry. In other words, the CIS Hamiltonian matrix, by construction, does not include any non-zero matrix elements coupling the ground state and any of the single excitations at *any* molecular geometry. This is a consequence of Brillouin's theorem, the restricted closed-shell ansatz, and the inclusion of only single excitations in the Hamiltonian matrix. The proper behaviour of the PESs around the intersection is shown in figure 8, using a SA-3-CAS(6/4) wavefunction. The degeneracy is split along the two directions shown and the conical nature of the intersection is evident.

Since TDDFT also does not include double excitations, as discussed above, behaviour similar to CIS may be expected. The PESs which result for the linear water molecule near the surface crossing are shown in figure 9.

Only one molecular displacement splits the degeneracy, as in CIS. However, there are further difficulties as alluded to in figure 6. Specifically, the response state energy varies much more rapidly than would be expected from the SA-3-CASSCF results shown in figure 8.

It is possible that these difficulties with TDDFT around conical intersection points would be resolved as long as the wavefunction ansatz used to generate the density was able to describe both interacting states around the intersection. A simple test case which satisfies this criterion is an intersection in H_3. In this case, both the ground and lowest excited states are doublet spin states and the quartet spin state is energetically well separated from these. Since the ground state is a spin doublet, an unrestricted Kohn–Sham formalism can be used. We have used both unrestricted and restricted open-shell (RO) TDDFT methods for this problem and the results are in semi-quantitative agreement. Hence, only the RO-TDDFT results are shown. In figure 10, the ground and excited state PESs around a MECI are shown using RO-TDDFT and CASSCF. Both methods show that the degeneracy is split along two molecular displacements, i.e. TDDFT correctly predicts the dimensionality of the intersection space. However, the problem of rapid variation of the response state energy in the region of the intersection remains.

We have also carried out comparisons of TDDFT and MS-CASPT2 in the region of S_1/S_2 conical intersections for several molecules including malonaldehyde and benzene. The dimensionality of the intersection space is correct in these cases and the rapid variation of the energy near the intersection is no longer observed. The detailed agreement of the MECI geometries between TDDFT and MS-CASPT2 is generally not as good as we show here for S_0/S_1 MECIs. However, it does not seem useful to pursue such comparisons until some of the basic problems we point out here are corrected.

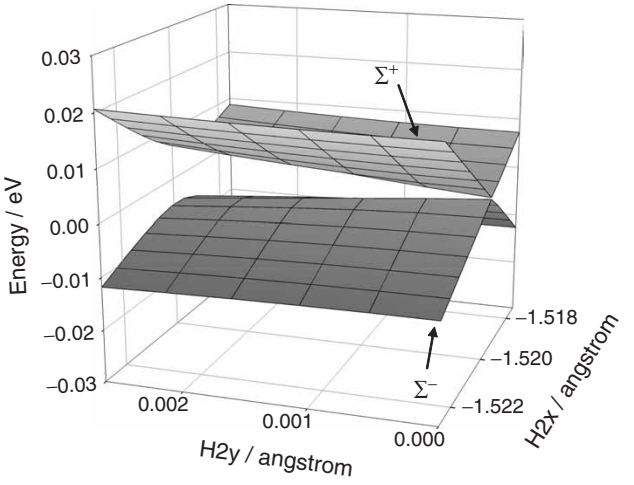

Figure 8. As in figure 7, but using SA3-CAS(6/4)/6-31G. The pronounced conical nature of the intersection is clear, in contrast to figure 7.

5. Discussion

We have shown that TDDFT does not include doubly-excited states in ethylene and butadiene. This is in contrast to previous speculation for butadiene based on vertical excitation energies. Investigation of the

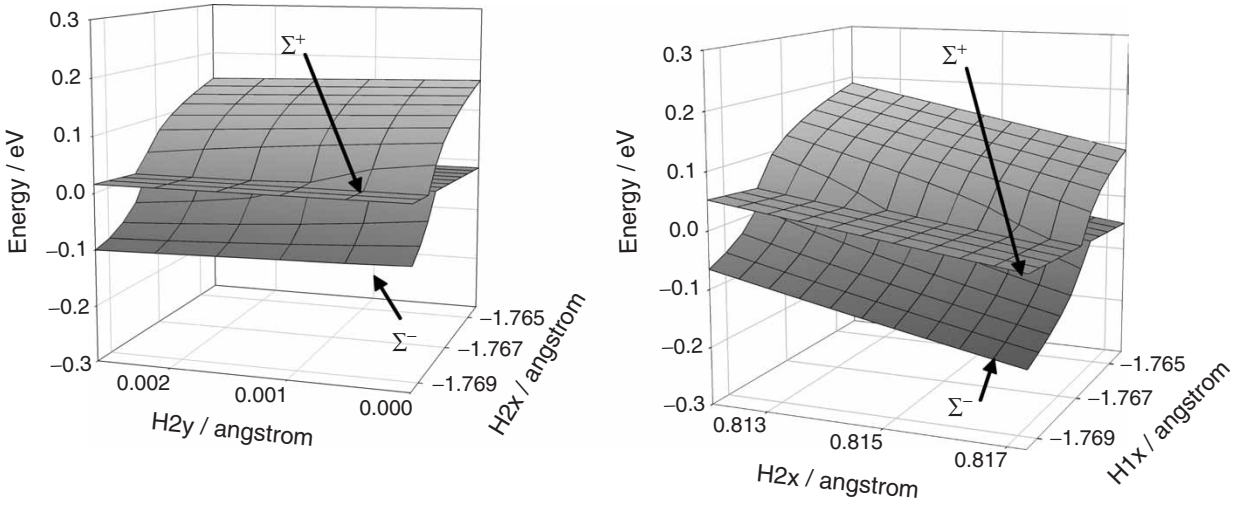

Figure 9. As in figure 7, but using TD-B3LYP/6-31G. As in CIS, only one branching direction is observed instead of the two which should be present. Furthermore, note the change in scale of the energy axis compared to figures 7 and 8.

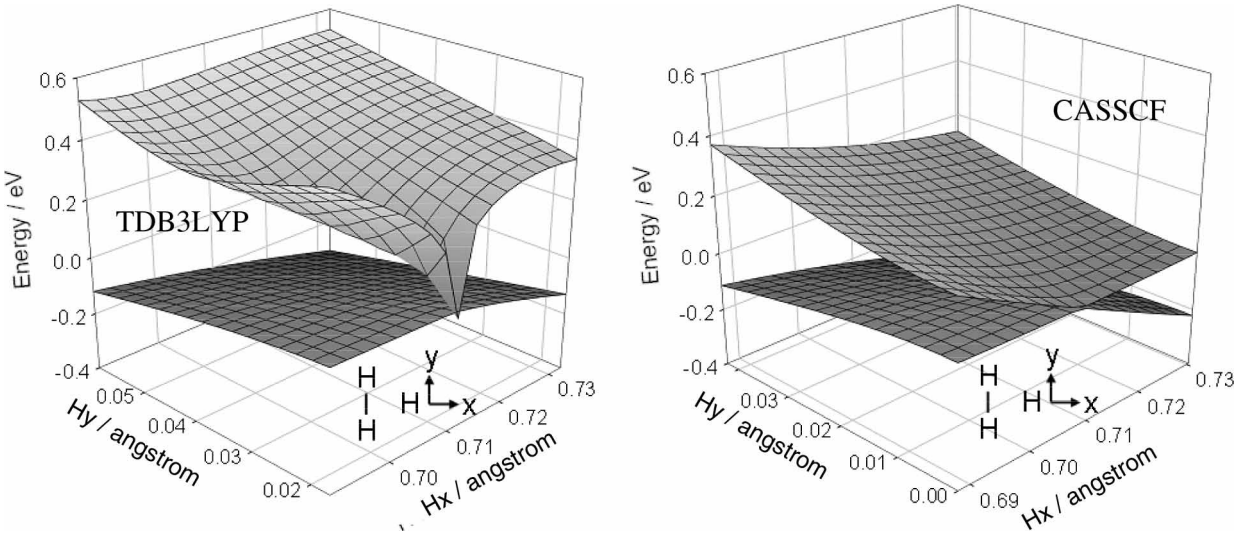

Figure 10. Comparison of PESs of $H_2 + H$ surrounding a conical intersection at CAS(3/3)/6-31G and TD-B3LYP/6-31G levels of theory. The molecule lies in the x–y plane, with the origin at the centre of the H_2 bond (distance fixed to 0.818 Å) and the y axis parallel to the H_2 bond. The position of the third hydrogen atom is varied along the x and y axes. In both cases, two directions split the degeneracy between the surfaces. This is in contrast to the comparison of figures 7–9, and arises because the ground and first excited state in TDDFT can both be represented by the wavefunction ansatz used to generate the density. However, the form of the excited state PES in TDDFT still exhibits unphysical rapid variation near the intersection as seen in figure 9.

global behaviour of the excited states of butadiene shows that a higher-lying singly-excited A_g state happens to be poorly predicted by TDDFT and appears in the energy range where the lowest A_g state (which should have a large amount of doubly-excited character) is expected. We have shown that states with predominant singly-excited character are well predicted by TDDFT even far outside the Franck–Condon region, at least for the chromophore of photoactive yellow protein. We introduced a new method for locating minimal energy conical intersections when the non-adiabatic coupling vector is not available and applied this to MS-CASPT2 and TDDFT. We showed that *conical* intersections involving a closed-shell singlet initial state cannot exist in TDDFT for the same reason they cannot exist in single-reference CIS—namely the interaction matrix elements connecting the initial state and response states are excluded from the formulation. This gives rise to surface intersections where only one molecular displacement breaks the degeneracy. Even when there are non-zero matrix elements connecting the initial and response states, the behaviour of TDDFT around intersections appears incorrect in that the variation of the response state energy is much more rapid than is found in *ab initio* treatments.

A few comments concerning the improvements necessary in TDDFT are in order. There are three distinct types of failures in linear response adiabatic TDDFT which are exemplified in this work. The first is the dimensionality of the intersection space, the second is the rapid variation of the energy of response states near intersections with the ground state, and the third is the lack of double excitations. The first problem comes when the wavefunction ansatz used to express the density is overly restrictive, i.e. it cannot describe both interacting states in the vicinity of the intersection. One possible solution is to express all states of interest as response states. The spin-flip (SF) TDDFT method is an example of such a strategy, using a reference state whose spin multiplicity is different from that desired [78]. Further inquiry into the ability of SF-TDDFT to describe conical intersections involving the ground state could be fruitful. Along similar lines, fractional occupation number (FON) methods may be appropriate [79, 80]. In this case, one can envision a response theory based on FON-DFT where both ground and excited states would be obtained from linear response applied to the ensemble density. This will likely require a modified exchange-correlation functional, as the reference state is essentially generated from the ensemble Kohn–Sham method [81].

We have no easy explanation for the observed rapid variation of the energy in the region of intersections. This could be related to deficiencies in the exchange correlation functional, but more likely is a consequence of the fact that an ensemble DFT procedure is required when the ground state is degenerate.

Double excitations can be incorporated in TDDFT either by extending the method beyond linear

response [82] or in a matrix-partitioning approach as developed by Burke and co-workers [13, 14]. It is interesting to note that SF-TDDFT can also solve this problem, but in a quite different way. As a specific example, consider ethylene, where the $m_s = 0$ component of the triplet spin state, which would be the target state determinant, is $|\pi\bar{\pi}^*\rangle$ and the presence/absence of the overbar denotes pairing with an α/β spin function. The three singlet states which are most important in the photochemistry of ethylene are $|\pi\bar{\pi}\rangle$, $|\pi^*\bar{\pi}^*$ and $|\pi\bar{\pi}^*\rangle + |\pi^*\bar{\pi}\rangle$. All three of these are generated as single excitations (where spin flipping is viewed as an excitation) from the target state. Hence, the double excitation is a response state treated on the same footing as the ground state and the singly-excited state.

The results of this study are mixed, but potentially promising. The behaviour of DFT in the region around conical intersections may provide a stringent test for future functionals and further motivation for the development of DFT methods which incorporate multireference character. Work along these lines is in progress.

Acknowledgements

The authors are pleased to acknowledge many lively discussions on the topics with Professors R. M. Martin, E. K. U. Gross, K. Burke and R. Cave. This work was supported by the National Science Foundation (CHE-02-311876 and DMR-03-25939) with additional support through the Frederick Seitz Materials Research Laboratory (DOE DEFG02-91ER45439) at the University of Illinois Urbana-Champaign. TJM is a Packard Fellow and a Dreyfus Teacher-Scholar. BGL is a Lubrizol Fellow. We thank NCSA for a generous grant of computing time.

References

[1] E. K. U. Gross and W. Kohn, Adv. Quantum Chem. **21,** 255 (1990).
[2] M. Petersilka, U. J. Gossmann, and E. K. U. Gross, Phys. Rev. Lett. **76,** 1212 (1996).
[3] H. Appel, E. K. U. Gross, and K. Burke, Phys. Rev. Lett. **90,** 043005 (2003).
[4] M. E. Casida, in *Recent Advances in Density Functional Methods*, edited by D. P. Chong (World Scientific, Singapore, 1995), Vol. 1, p. 155.
[5] E. Runge and E. K. U. Gross, Phys. Rev. Lett. **52,** 997 (1984).
[6] N. C. Handy and D. J. Tozer, J. Comput. Chem. **20,** 106 (1999).
[7] T. Grabo, M. Petersilka, and E. K. U. Gross, J. Molec. Struct. (THEOCHEM) **501,** 353 (2000).
[8] D. J. Tozer, R. D. Amos, N. C. Handy, B. O. Roos, and L. Serrano-Andres, Molec. Phys. **97,** 859 (1999).
[9] J. Guan, M. E. Casida, and D. R. Salahub, J. Molec. Struct. (THEOCHEM) **527,** 229 (2000).
[10] D. J. Tozer and N. C. Handy, J. Chem. Phys. **109,** 10180 (1998).
[11] M. E. Casida, C. Jamorski, K. C. Casida, and D. R. Salahub, J. Chem. Phys. **108,** 4439 (1998).
[12] M. E. Casida and D. R. Salahub, J. Chem. Phys. **113,** 8918 (2000).
[13] N. T. Maitra, F. Zhang, R. J. Cave, and K. Burke, J. Chem. Phys. **120,** 5932 (2004).
[14] R. J. Cave, F. Zhang, N. T. Maitra, and K. Burke, Chem. Phys. Lett. **389,** 39 (2004).
[15] C.-P. Hsu, S. Hirata, and M. Head-Gordon, J. Phys. Chem. A **105,** 451 (2001).
[16] M. E. Casida, F. Gutierrez, J. Guan, F.-X. Gadea, D. R. Salahub, and J.-P. Daudey, J. Chem. Phys. **113,** 7062 (2000).
[17] A. Dreuw and M. Head-Gordon, J. Am. Chem. Soc. **126,** 4007 (2004).
[18] S. Grimme and M. Parac, Chem. Phys. Chem. **4,** 292 (2003).
[19] A. Dreuw, J. L. Weisman, and M. Head-Gordon, J. Chem. Phys. **119,** 2943 (2003).
[20] M. E. Casida, K. C. Casida, and D. R. Salahub, Int. J. Quantum Chem. **70,** 933 (1998).
[21] M. Wanko, M. Garavelli, F. Bernardi, T. A. Niehaus, T. Frauenheim, and M. Elstner, J. Chem. Phys. **120,** 1674 (2004).
[22] M. Ben-Nun and T. J. Martínez, Chem. Phys. **259,** 237 (2000).
[23] D. R. Yarkony, Acc. Chem. Res. **31,** 511 (1998).
[24] M. A. Robb, F. Bernardi, and M. Olivucci, Pure Appl. Chem. **67,** 783 (1995).
[25] M. Klessinger and J. Michl, *Excited States and Photochemistry of Organic Molecules* (VCH Publishers, New York, 1995).
[26] M. Ben-Nun, J. Quenneville, and T. J. Martínez, J. Phys. Chem. A **104,** 5161 (2000).
[27] K. K. Docken and J. Hinze, J. Chem. Phys. **57,** 4928 (1972).
[28] B. O. Roos, in *Advances in Chemical Physics:* ab initio *Methods in Quantum Chemistry II*, edited by K. P. Lawley (Wiley, New York, 1987), p. 399.
[29] M. J. Bearpark, M. Deumal, M. A. Robb, T. Vreven, N. Yamamoto, M. Olivucci, and F. Bernardi, J. Am. Chem. Soc. **119,** 709 (1997).
[30] F. Bernardi, A. Bottoni, M. Olivucci, A. Venturini, and M. A. Robb, Faraday Trans. **90,** 1617 (1994).
[31] F. Bernardi, M. Olivucci, M. A. Robb, T. Vreven, and J. Soto, J. Org. Chem. **65,** 7847 (2000).
[32] P. Celani, F. Bernardi, M. Olivucci, and M. A. Robb, J. Chem. Phys. **102,** 5733 (1995).
[33] P. Celani, S. Ottani, M. Olivucci, F. Bernardi, and M. A. Robb, J. Am. Chem. Soc. **116,** 10141 (1994).
[34] M. Garavelli, P. Celani, F. Bernardi, M. A. Robb, and M. Olivucci, J. Am. Chem. Soc. **119,** 6891 (1997).
[35] M. Garavelli, P. Celani, M. Fato, M. J. Bearpark, B. R. Smith, M. Olivucci, and M. A. Robb, J. Phys. Chem. A **101,** 2023 (1997).

[36] B. O. Roos, Acc. Chem. Res. **32,** 137 (1999).
[37] T. Vreven, F. Bernardi, M. Garavelli, M. Olivucci, M. A. Robb, and H. B. Schlegel, J. Am. Chem. Soc. **119,** 12687 (1997).
[38] L. Blancafort, P. Hunt, and M. A. Robb, J. Am. Chem. Soc. **127,** 3391 (2005).
[39] J. C. Tully, J. Chem. Phys. **93,** 1061 (1990).
[40] J. C. Tully and R. K. Preston, J. Chem. Phys. **55,** 562 (1971).
[41] M. Ben-Nun and T. J. Martinez, Adv. Chem. Phys. **121,** 439 (2002).
[42] M. Ben-Nun and T. J. Martínez, J. Am. Chem. Soc. **122,** 6299 (2000).
[43] C. Ko, B. Levine, A. Toniolo, L. Manohar, S. Olsen, H.-J. Werner, and T. J. Martinez, J. Am. Chem. Soc. **125,** 12710 (2003).
[44] T. J. Martínez, Chem. Phys. Lett. **272,** 139 (1997).
[45] T. Schultz, J. Quenneville, B. Levine, A. Toniolo, T. J. Martinez, S. Lochbrunner, M. Schmitt, J. P. Shaffer, M. Z. Zgierski, and A. Stolow, J. Am. Chem. Soc. **125,** 8098 (2003).
[46] H. Choi, K. K. Baeck, and T. J. Martinez, Chem. Phys. Lett. **398,** 407 (2004).
[47] K. K. Baeck and T. J. Martinez, Chem. Phys. Lett. **375,** 299 (2003).
[48] T. Kreibich and E. K. U. Gross, Phys. Rev. Lett. **86,** 2984 (2001).
[49] J. B. Foresman, M. Head-Gordon, J. A. Pople, and M. J. Frisch, J. Phys. Chem. **96,** 135 (1992).
[50] J. Finley, P.-A. Malmqvist, B. O. Roos, and L. Serrano-Andres, Chem. Phys. Lett. **288,** 299 (1998).
[51] P. Hohenberg and W. Kohn, Phys. Rev. B **136,** 864 (1964).
[52] N. T. Maitra and K. Burke, Phys. Rev. A **63,** 042501 (2001).
[53] N. T. Maitra, K. Burke, and C. Woodward, Phys. Rev. Lett. **89,** 023002 (2002).
[54] S. Hirata and M. Head-Gordon, Chem. Phys. Lett. **314,** 291 (1999).
[55] R. E. Stratmann, G. E. Scuseria, and M. J. Frisch, J. Chem. Phys. **109,** 8218 (1998).
[56] M. Ben-Nun and T. J. Martínez, Chem. Phys. Lett. **298,** 57 (1998).
[57] W. G. Dauben, L. Salem, and N. J. Turro, Acc. Chem. Res. **8,** 41 (1975).
[58] J. Quenneville, M. Ben-Nun, and T. J. Martínez, J. Photochem. Photobiol. A **144,** 229 (2001).
[59] M. W. Schmidt, K. K. Baldridge, J. A. Boatz, S. T. Elbert, M. S. Gordon, J. H. Jensen, S. Koseki, N. Matsunaga, K. A. Nguyen, S. J. Su, T. L. Windus, M. Dupuis, and J. A. Montgomery, J. Comput. Chem. **14,** 1347 (1993).
[60] M. J. Frisch, G. W. Trucks, H. B. Schlegel, G. E. Scuseria, M. A. Robb, J. R. Cheesman, V. G. Zakrzewski, J. A. Montgomery Jr, R. E. Stratmann, J. C. Burant, S. Dapprich, J. M. Millam, A. D. Daniels, K. N. Kudin, M. C. Strain, O. Farkas, J. Tomasi, B. Barone, M. Cossi, R. Cammi, B. Mennucci, C. Pomelli, C. Adamo, S. Clifford, J. Ochterski, G. A. Petersson, P. Y. Ayala, Q. Cui, K. Morokuma, D. K. Malick, A. D. Rabuck, K. Raghavachari, J. B. Foresman, J. Cioslowski, J. V. Oritiz, B. B. Stefanov, G. Liu, A. Liashenko, P. Piskorz, I. Komaromi, R. Gomperts, R. L. Martin, D. J. Fox, T. Keith, M. A. Al-Laham, C. Y. Peng, A. Nanayakkara, C. Gonzalez, M. Challacombe, P. M. W. Gill, B. Johnson, W. Chen, M. W. Wong, J. L. Andres, C. Gonzalez, M. Head-Gordon, E. S. Replogle, and J. A. Pople, Gaussian 98, revision A.1 ed. (Gaussian, Inc., Pittsburgh, 1998).
[61] L. Serrano-Andres, M. Merchan, I. Nebot-Gil, R. Lindh, and B. O. Roos, J. Chem. Phys. **98,** 3151 (1993).
[62] R. L. Graham and K. F. Freed, J. Chem. Phys. **96,** 1304 (1992).
[63] R. J. Cave, K. Burke, and E. W. Castner, J. Phys. Chem. A **106,** 9294 (2002).
[64] H.-J. Werner and P. J. Knowles, with contributions from R. D. Amos, A. Bernhardsson, A. Berning, P. Celani, D. L. Cooper, M. J. O. Deegan, A. J. Dobbyn, F. Eckert, C. Hampel, G. Hetzer, P. J. Knowles, T. Korona, R. Lindh, A. W. Lloyd, S. J. McNicholas, F. R. Manby, W. Meyer, M. E. Mura, A. Nicklass, P. Palmieri, R. Pitzer, G. Rauhut, M. Schütz, U. Schumann, H. Stoll, A. J. Stone, R. Tarroni, T. Thorsteinsson, H.-J. Werner, MOLPRO, version 2002.2 (2002), a package of *ab initio* programs, see http://www.molpro.net
[65] W. H. Press, S. A. Teukolsky, W. T. Vetterling, and B. P. Flannery, *Numerical Recipes in FORTRAN* (Cambridge Press, Cambridge, 1992).
[66] M. J. Bearpark, M. A. Robb, and H. B. Schlegel, Chem. Phys. Lett. **223,** 269 (1994).
[67] M. R. Manaa and D. R. Yarkony, J. Chem. Phys. **99,** 5251 (1993).
[68] R. Baer, Chem. Phys. Lett. **364,** 75 (2002).
[69] V. Chernyak and S. Mukamel, J. Chem. Phys. **112,** 3572 (2000).
[70] R. Fletcher, *Practical Methods of Optimization* (Wiley, New York, 2000).
[71] M. Olivucci, I. N. Ragazos, F. Bernardi, and M. A. Robb, J. Am. Chem. Soc. **115,** 3710 (1993).
[72] M. Garavelli, F. Bernardi, M. Olivucci, M. J. Bearpark, S. Klein, and M. A. Robb, J. Phys. Chem. A **105,** 11496 (2001).
[73] J. Quenneville and T. J. Martínez, J. Phys. Chem. A **107,** 829 (2003).
[74] M. Ben-Nun, F. Molnar, K. Schulten, and T. J. Martínez, Proc. Natl. Acad. Sci. **99,** 1769 (2002).
[75] D. R. Yarkony, J. Chem. Phys. **114,** 2601 (2001).
[76] G. J. Atchity, S. S. Xantheas, and K. Ruedenberg, J. Chem. Phys. **95,** 1862 (1991).
[77] D. R. Yarkony, Rev. Mod. Phys. **68,** 985 (1996).
[78] Y. Shao, M. Head-Gordon, and A. I. Krylov, J. Chem. Phys. **118,** 4807 (2003).
[79] S. G. Wang and W. H. E. Schwarz, J. Chem. Phys. **105,** 4641 (1996).
[80] B. I. Dunlap and W. N. Mei, J. Chem. Phys. **78,** 4997 (1983).
[81] N. I. Gidopoulos, P. G. Papaconstantinou, and E. K. U. Gross, Phys. Rev. Lett. **88,** 033003 (2002).
[82] K. Yabana and G. F. Bertsch, Int. J. Quantum Chem. **75,** 55 (1999).